Calculation of x-ray magnetic circular dichroism in Gd

A. Ankudinov and J. J. Rehr
Department of Physics, University of Washington, Seattle, Washington 98195-1560
(Received 7 March 1995)

An approximate theory for x-ray magnetic circular dichroism (XMCD) is presented for the special case of half-filled shells, e.g., Gd. The L_2 and L_3 XMCD structure arises primarily from the exchange interaction of the photoelectron and provides a test of various exchange models. The XMCD signal can be interpreted in terms of an effective magnetic scattering amplitude that depends on the spin of the absorber and of the scattering atoms. *Ab initio* curved-wave multiple-scattering calculations for the L_2 and L_3 edges of Gd are found to be in satisfactory agreement with experiment.

I. INTRODUCTION

X-ray magnetic circular dichroism (XMCD) in the x-ray-absorption near-edge structure (XANES) region, i.e., for photoelectron energies within about 10 eV of threshold, was predicted by Erskine and Stern.[1] Much experimental and theoretical work has recently been carried out on XMCD in this region,[2–7] where the main mechanism responsible for the XMCD signal is the filling of different m_l states.[1] There has also been considerable interest in sum rules for the XMCD signal.[4] A complete set of such sum rules has been derived.[5] Such sum rules have been used to determine contributions from orbital and spin angular momenta to the net magnetization.[4] With improved synchrotron x-ray sources, XMCD data in the extended x-ray-absorption fine structure (EXAFS) region, i.e., 10–1000 eV above threshold, has also become available.[2] We shall refer to this extended fine-structure signal as circular polarized x-ray-absorption fine structure (CPXAFS); it is also referred to as spin-polarized extended XAFS (SPEXAFS).[2] Unlike the situation near threshold, all m_l states are unoccupied far from the edge and are equally available for transitions. Therefore different mechanisms, e.g., exchange and spin-orbit (SO) interactions, must be sought for the XMCD signal at high energies.

In this paper we present a quantitative theory of XMCD, especially above the L_2 and L_3 edges of Gd in EXAFS region. For these edges we argue that the photoelectron exchange interaction is primarily responsible for the CPXAFS. This is borne out by the reasonable agreement between the calculated signal and experiment. This also suggests that XMCD measurements provide a significant test of various exchange-correlation potentials.

II. XMCD FOR HALF-FILLED SHELLS

For simplicity, we treat in this paper the special case of half-filled shells (e.g., Gd), so that spherical symmetry of the scattering potential is retained. One source of XMCD in this model is the SO interaction of core electrons. When $l \neq 0$, this interaction affects the relative alignment of the spin and angular momentum of core electrons. By examining the appropriate dipole matrix elements, one sees that right circular polarized (RCP) light, $\Delta m = +1$, produces more photoelectrons with a positive projection of angular momentum $\langle L_z \rangle$ along the magnetic field, $\mathbf{B} = B\hat{\mathbf{z}}$, and conversely left circular polarized (LCP) light, $\Delta m = -1$, produces more with a negative projection. Thus for $j = l + 1/2$, RCP x rays will produce more spin-up electrons. This is analogous to the well-known Fano effect[8] of atomic physics. A second source of XMCD in magnetic materials is the photoelectron exchange interaction or self-energy V_{xc}. Spin-up ($\uparrow$) and spin-down ($\downarrow$) photoelectrons have different scattering potentials due to different exchange interactions with the different spin populations. This leads to different backscattering amplitudes for spin-up and -down photoelectrons, and hence a XMCD signal due to a difference in the XAFS spectra for RCP and LCP light. Furthermore we will make the additional but reasonable approximations of neglecting the exchange splitting of the core levels and the SO interaction of the photoelectron. The latter interaction is usually an order of magnitude less important than exchange. A similar model has been used by Ebert and co-workers to calculate the near-edge XMCD spectrum.[7]

The average $\langle L_z \rangle$ in magnetic materials is nonzero, except for elements with half-filled core levels. However, if one maintains the spherical symmetry of the atomic scattering problem, the spherically symmetric scattering potential and phase shifts will still depend on the values of m_l and m_s of the photoelectron. This dependence requires some knowledge of the ground-state electronic configuration (i.e., the ground-state density matrix), but otherwise can be included in a straightforward generalization of the multiple-scattering (MS) formalism of x-ray absorption. For half-filled configurations, the scattering potential is different for spin-up and -down electrons but independent of m_l. Our present codes can also be used as a first approximation for other than half-filled configurations in a simplified model of the density matrix which assumes equally populated L_z states with the same spin direction. This will give the correct total spin, as in Hund's

0163-1829/95/52(14)/10214(7)/$06.00

rule, but the wrong $\langle L_z \rangle$ (except for the half-filled case). Thus we assume that all spins are aligned along the z axis (i.e., as in a ferromagnet far below T_c), and temperature independent. The spin of the photoelectron can be regarded as a conserved quantity because we neglect the SO interaction of the photoelectron. Also because this SO interaction is neglected, this model predicts no XMCD signal for $l = 0$ shells in the dipole approximation.[9] However, two other mechanisms that neglect SO must be considered. First, as noted above, RCP light will produce more photoelectrons with positive m_l, which have different exchange interactions with partly filled valence shells. Second, if one neglects the difference in m_l filling of valence shells but includes magnetic dipole transitions, then RCP light will produce only spin-up electrons due to these transitions and hence a nonzero XMCD signal. On the other hand, Brouder[10] has argued that the magnetic dipole effect is small and observations have convincingly failed to observe any effect.[11] The exchange splitting at the $l = 0$ edge may also be important. For example, this splitting is 6.7 eV at the M_1 edge of Mn in $KMnF_3$.[12] A more detailed treatment of the $l = 0$ case is given by Brouder *et al.*[10]

Below we develop a quantitative MS theory for XMCD and CPXAFS for $l \neq 0$ shells based on these considerations. The formal treatment of Brouder and Hikam is similar.[9] However, these authors have not carried out explicit calculations, and they make some approximations in the expression for the XMCD fine structure which are not always justified. In particular, we find that the atomic matrix element dependence of the fine structure is essential to achieve agreement with experiment. Our treatment makes use of the fast Rehr-Albers (RA) MS formalism[13] and takes advantage of symmetry properties of the total propagator G. This leads to feasible calculations from threshold to $k = 20$ Å^{-1} based on a straightforward generalization of the *ab initio* polarized MS XAFS code FEFF (version 6).[14]

Using the Green's-function formalism of RA,[13] we can write the absorption of RCP (+) and LCP (−) light from core level j and angular momentum l within one-particle theory as

$$\mu^{\pm}(k) = -\frac{A\,k_0}{\pi}\,\mathrm{Im} \sum_{L_n, L_0, m_s} G^{m_s}_{L_n, L_0} \sum_{m_j} \langle J| - \left(p_{\mp} + \frac{i}{2} k_0^2 z \sigma_{\mp}\right) |L_n S\rangle \langle L_0 S| p_{\pm} - \frac{i}{2} k_0^2 z \sigma_{\pm} |J\rangle. \tag{1}$$

Here we have also included the leading term from magnetic dipole interaction, which is negligible except possibly for the K, L_1, and M_1 shells. In what follows the indices j and l will not be indicated explicitly unless otherwise needed for clarity. In Eq. (1) the momentum operator is $p_+ = -(p_x + i p_y)/\sqrt{2}$, $\Delta m = +1(-1)$ for RCP(LCP) light [we follow the notation for vector components $V_{\pm}$ and phase conventions of Messiah[15] (see p. 1075), which are consistent with the Racah definitions], $k = \sqrt{2(E - E_0)}$ is the photoelectron wave number defined with respect to the threshold energy E_0 [we use atomic units $e = \hbar = m = 1$], $k_0 = \omega/c$ is the photon wave number (or energy), $A = 1/2\pi c$ in atomic units; any L is an abbreviation for the angular quantum numbers (l, m_l), $S = (1/2, m_s)$, and $J = (j, m_j)$; L_n and L_0 are the final state and initial state orbital angular momenta of the photoelectron, respectively; and $G^{m_s}_{L_n, L_0} = \langle L_n \mathbf{0} | G^{m_s} | L_0 \mathbf{0} \rangle$ is the matrix element of the total propagator between these angular momentum and absorption site states (henceforth, we suppress the site index). In the MS expansion, the total propagator is given by the sum over contributions from all distinguishable MS paths Γ defined by the path leg vectors $\mathbf{R}_1, \mathbf{R}_2 \ldots \mathbf{R}_n$ that leave and return to the absorbing site:

$$G^{m_s}_{L_n, L_0} = G^{c, m_s}_{L_n, L_0} + \sum_{\Gamma} G^{(n-1), m_s}_{L_n, L_0}(\Gamma) e^{i\delta^c_{l_n, m_s} + i\delta^c_{l_0, m_s}}, \tag{2}$$

where $G^{c, m_s}_{L_n, L_0}$ is the central atom Green's function. An expression for $G^{(n-1)}_{L_n, L_0}(\Gamma)$ is given by Eq. (15) of RA, but now is different for different $m_s = \pm 1/2$ and different $j = j^{\pm} = l \pm 1/2$. For clarity, to differentiate between x-ray polarization and photoelectron spin, we will use the notation $\uparrow$ ($\downarrow$) for spin $m_s = +1/2(-1/2)$ and $+(-)$ for RCP (LCP) light.

The main contribution to the absorption $\mu(k)$ comes from the $l \to l+1$ transition ($l_0 = l_n$). From conservation of the projection of angular momentum, $m_0 + m_s = m_j + 1 = m_n + m_s$, it follows that $m_0 = m_n$, and

$$\begin{aligned} \mu^{+}(k) = -\frac{A\,k_0}{\pi}\,\mathrm{Im} & \\ \times \sum_{L_n, m_s} G^{m_s}_{L_n, L_n} \sum_{m_j} & \langle J | L\,S \rangle \langle L\,S | p_- | L_n\,S \rangle \\ \times \langle L_n\,S | p_+ | L\,S \rangle & \langle L\,S | J \rangle, \end{aligned} \tag{3}$$

where $\langle L\,S | J \rangle$ are Clebsch-Gordon coefficients.[15] Using the Wigner-Eckart theorem for dipole matrix elements we obtain

$$\begin{aligned} \mu^{+}(k) = -\frac{1}{\pi}\mathrm{Im} \sum_{m_n, m_s} & G^{m_s}_{L_n, L_n} \Delta^2_{m_s} \\ \times \sum_{m_j, m_l} & (2j+1) \begin{pmatrix} j & l & 1/2 \\ -m_j & m_l & m_s \end{pmatrix}^2 \\ \times & \begin{pmatrix} l & 1 & l+1 \\ m_l & +1 & -m_n \end{pmatrix}^2, \end{aligned} \tag{4}$$

where the reduced matrix element $\Delta_{m_s} = \sqrt{A\,k_0}|\langle l\,j || p || l+1, m_s \rangle|$ depends on j, because the initial state radial wave function differs for $j = j^{\pm}$, and the final state radial wave function depends on m_s. The difference in the result for $\mu^{-}(k)$ is only a sign change, with -1 in the second $3j$ symbol instead of $+1$. Using invari-

ance of $3j$ symbols under the simultaneous sign change of all m_i, we obtain

$$\mu^-(k) = -\frac{1}{\pi}\mathrm{Im}\sum_{m_n,m_s} G^{-m_s}_{l_n\,-m_n,l_n\,-m_n}\Delta^2_{-m_s} \times \sum_{m_j,m_l}(2j+1)\begin{pmatrix} j & l & 1/2 \\ -m_j & m_l & m_s\end{pmatrix}^2 \times \begin{pmatrix} l & 1 & l+1 \\ m_l & +1 & -m_n\end{pmatrix}^2. \quad (5)$$

Diagonal elements of the propagator have the property that $G_{l\,-m,l\,-m} = G_{l\,m,l\,m}$, which follows from the symmetry of $g^{|\mu|}_{l1,l2} = g^{|\mu|}_{l2,l1}$ [RA, Eq. (10)] and the properties of rotation matrices,[15] $R^l_{m_1,m_2}(\Omega^{-1}_{\hat{\rho}}) = (-1)^{m_2-m_1}R^l_{m_2,m_1}(\Omega_{\hat{\rho}})$ substituted into Eq. (9) of RA.[13] Here $\Omega_{\hat{\rho}}$ refers to the Euler angles that rotate a bond ρ onto the z-axis. For identical superscripts, which are henceforth suppressed, this procedure gives $G_{l_1\,-m_1,l_2\,-m_2} = (-1)^{m_2-m_1}G_{l_2\,m_2,l_1\,m_1}$. Thus in Eq. (14) of RA, the contribution to $G_{lm,lm}$ from the path $\Gamma = \mathbf{R}_1,\mathbf{R}_2\ldots\mathbf{R}_n$ is the same as the contribution to $G_{l\,-m,l\,-m}$ from the inverse path, $\Gamma^{-1} = \mathbf{R}_n,\mathbf{R}_{n-1}\ldots\mathbf{R}_1$. We therefore obtain for the XMCD signal from a subshell j,

$$\mu^+ - \mu^- = -\frac{1}{\pi}\mathrm{Im}\sum_{m_n,m_s}\left[G^{m_s}_{L_n,L_n}\Delta^2_{m_s} - G^{-m_s}_{L_n,L_n}\Delta^2_{-m_s}\right] \times \sum_{m_j,m_l}(2j+1)\begin{pmatrix} j & l & 1/2 \\ -m_j & m_l & m_s\end{pmatrix}^2 \times \begin{pmatrix} l & 1 & l+1 \\ m_l & +1 & -m_n\end{pmatrix}^2. \quad (6)$$

The second sum actually consists of just one term since $m = m_l + m_s$ and $m_n = m_l + 1$. Using properties of $3j$ symbols,[15] the sum over m_s gives,

$$\mu^+ - \mu^- = -\frac{1}{\pi}\mathrm{Im}\sum_{m_n}\left[G^{\uparrow}_{L_n,L_n}\Delta^2_{\uparrow} - G^{\downarrow}_{L_n,L_n}\Delta^2_{\downarrow}\right] \times \frac{(-1)^{(j-j^+)}\,l}{3(2l+3)(2l+1)}\,C(m_n), \quad (7)$$

where

$$C(m) = \frac{3(m-1)(l+m)(l+m+1)}{l(2l+1)(l+1)}. \quad (8)$$

If we now sum contributions from $j^{\pm}$ and neglect the j dependence of the propagators and matrix elements, Eq. (7) gives zero signal due to the $(-1)^j$ factor. From physical considerations alone we expect to have zero XMCD signal when the SO splitting of the $j^{\pm}$ shells is zero, because then there is no connection between electron-spin polarization and photon polarization. In order to take advantage of path symmetries, we can make use of the path-reversal symmetry property of G_{L_1,L_2} above and cancel out all odd powers of m,

$$C(m) = \frac{3(2m^2-l-1)}{(2l+1)(l+1)}. \quad (9)$$

In addition to (a) path-reversal symmetry, $(\Gamma \to \Gamma^{-1})$, paths give the same contribution to the total propagator if they take one into another under the operations of (b) rotations of any angle about the magnetization axis, and (c) reflections in the planes containing the magnetization axis and normal to it. These symmetries ignore the small phase shift due to magnetic flux.

In order to take advantage of the XAFS code FEFF6 to calculate the XMCD signal χ^M, it is convenient to define a normalized, spin-dependent XAFS function,

$$\chi^M_{m_s} = -\frac{1}{\pi}\mathrm{Im}\sum_{m_n,\Gamma}\frac{C(m_n)}{2l+3}G^{m_s}_{L_n,L_n}(\Gamma)e^{2i\delta^c_{l_n,m_s}}, \quad (10)$$

as FEFF is designed to calculate the full propagator $G^{m_s}_{L_n,L_n}(\Gamma)e^{2i\delta^c_{l_n,m_s}}$ using the MS expansion. It is convenient at this point to distinguish several different quantities that appear in the XMCD formalism. In this work we will use as normalization factors the atomic cross sections (denoted with a superscript A),

$$\mu^A = \frac{1}{2}(\mu^A_{\uparrow} + \mu^A_{\downarrow}) = -\frac{1}{\pi}\mathrm{Im}\,\frac{2j+1}{6(2l+1)}\left[G^{c,\uparrow}_{l\,0,l\,0}\Delta^2_{\uparrow} + G^{c,\downarrow}_{l\,0,l\,0}\Delta^2_{\downarrow}\right]. \quad (11)$$

The XMCD signal in Eq. (7) (denoted with superscript M) can be expressed as

$$\mu^M = \mu^+ - \mu^- = \mu^M_0 + \mu^M_S, \quad (12)$$

where μ^M_0 is the nearly smooth XMCD background arising from absorption within the central atom,

$$\mu^M_0 = \frac{(-1)^{(j-j^+)}\,l}{(2j+1)}\left(\mu^A_{\uparrow} - \mu^A_{\downarrow}\right), \quad (13)$$

and μ^M_S is the oscillating part of the XMCD signal, arising as in XAFS, from scattering by neighboring atoms,

$$\mu^M_S = \frac{(-1)^{(j-j^+)}\,l}{(2j+1)}\left[\mu^A_{\uparrow}\chi^M_{\uparrow} - \mu^A_{\downarrow}\chi^M_{\downarrow}\right]. \quad (14)$$

Because the matrix element factors $\mu^A_{\uparrow\downarrow}$ are spin dependent, the net XMCD effect is not simply due to the difference in $\chi^M_{\uparrow\downarrow}$. Similarly, the average XAFS signal from subshell j contains atomic matrix element factors and is given by

$$\Delta\mu = \frac{1}{3}(\mu^0 + \mu^+ + \mu^-) - \mu^A = \frac{1}{2}\left[\mu^A_{\uparrow}\chi_{\uparrow} + \mu^A_{\downarrow}\chi_{\downarrow}\right] = \frac{-1}{\pi}\frac{(2j+1)}{6(2l+1)(2l+3)}\mathrm{Im} \times \sum_{m_n}\left[G^{\uparrow}_{L_n,L_n}e^{2i\delta^c_{l_n,\uparrow}}\Delta^2_{\uparrow} + G^{\downarrow}_{L_n,L_n}e^{2i\delta^c_{l_n,\downarrow}}\Delta^2_{\downarrow}\right]. \quad (15)$$

Experimentally a factor close to -2 has been found between the XMCD signals above the L_2 and L_3 edges.[16]

This can be understood as follows. If one neglects the difference between the $j^{\pm}$ core wave functions, which is generally a good approximation, the following approximate results are obtained in terms of a generalized XAFS function $\chi_j = \Delta\mu_j/\mu_j^A$:

$$\begin{aligned}
\mu_{j^+}^A(k) &\approx \frac{l+1}{l}\mu_{j^-}^A(k), \\
\Delta\mu_{j^+}(k) &\approx \frac{l+1}{l}\Delta\mu_{j^-}(k), \\
\chi_{j^+}(k) &\approx \chi_{j^-}(k), \\
\mu_{j^+}^M(k) &\approx -\mu_{j^-}^M(k), \\
\chi_{j^+}^M(k) &\approx -\frac{l}{l+1}\chi_{j^-}^M(k).
\end{aligned} \tag{16}$$

Here

$$\chi_j^M \approx \frac{(-1)^{(j-j^+)}\,l}{(2j+1)}\left(\chi_\uparrow^M - \chi_\downarrow^M\right), \tag{17}$$

which should not be confused with $\chi_{m_s}^M$. Thus for $L_2(j = 1/2)$ and $L_3(j = 3/2)$ final states (both $l = 1$), we obtain a factor of precisely -2.

For polycrystalline materials, averaging over all directions leads to $C(m) = 1$ and hence from Eq. (10), $\chi_{\uparrow\downarrow}^M = \chi_{\uparrow\downarrow}$. This averaging significantly increases path symmetry and Eqs. (10)–(14) simplify to a very compact form for the XMCD, namely

$$\mu^M = \mu^+ - \mu^- = \frac{(-1)^{j-j^+}\,l}{(2j+1)}\left(\mu_\uparrow - \mu_\downarrow\right). \tag{18}$$

We can then use *unpolarized* FEFF6 calculations to obtain the XMCD signal. Here $\mu_{\uparrow\downarrow} = \mu_{\uparrow\downarrow}^A(1 + \chi_{\uparrow\downarrow})$ is the net j-edge absorption coefficient calculated with the potential for spin-up and -down electrons, respectively. This formula explicitly connects the XMCD signal to the spin polarization of the system. However, within the dipole approximation, the result gives no XMCD signal in nonmagnetic systems.

One can estimate the magnitude of the XMCD signal for polycrystalline materials using the single-scattering approximation and neglecting the difference between the background amplitudes $\mu_{\uparrow\downarrow}^A$. Then, using the exact curved-wave expression (or somewhat less accurately, the spherical wave approximation)[13] for the scattering amplitude at site i in Eqs. (10)–(14), one obtains $G_{L,L} \approx \sum_i (e^{2i\rho_i}/\rho_i^2) f_i^{m_s}(\pi) e^{2i\delta_{l,m_s}^c}$, where the sum is over all neighbors to the absorber and $\rho_i = kR_i$:

$$\begin{aligned}
\mu_S^M \approx \mathrm{Im}&\frac{(-1)^{j-j^+}\,l}{(2j+1)}\mu^A \\
&\times \sum_i \frac{e^{2i\rho_i}}{\rho_i^2}\left[f_i^\uparrow(\pi)e^{2i\delta_{l_n,\uparrow}^c} - f_i^\downarrow(\pi)e^{2i\delta_{l_n,\downarrow}^c}\right].
\end{aligned} \tag{19}$$

The term in square brackets can be interpreted as an effective magnetic scattering amplitude

$$f_{\mathrm{eff}}^M = f_i^\uparrow(\pi)e^{2i\delta_{l_n,\uparrow}^c} - f_i^\downarrow(\pi)e^{2i\delta_{l_n,\downarrow}^c}. \tag{20}$$

Note that f_{eff}^M arises partly from the magnetization of the scattering atom and partly from the central atom phase shift. Comparison of f_{eff}^M and the corresponding nonmagnetic scattering amplitude f_{eff} of XAFS shows that for Gd, f_{eff}^M is smaller by a factor which varies roughly inversely with k and out of phase by about $\pi/2$. One interpretation for this behavior is the derivative effect of the exchange energy difference between up- and down-spin populations; i.e., $(d\chi/dE)\Delta E \sim i\Delta E/k$. This result also explains the comparatively small amplitude of the XMCD signal at large photoelectron energies.

We can use Eq. (18) to calculate the XMCD signal for Gd because the L_2-L_3 separation is approximately 700 eV and the two signals are well separated. However, when the SO splitting is small, for example in Mn where the L_2-L_3 splitting is 10 eV, one must sum over contributions from both $j^{\pm}$ channels. We can also neglect the difference between matrix elements for $j = l \pm 1/2$ electrons (and the same core orbital wave function) since this is a good approximation when the SO interaction is small. Then the propagators differ only by a constant shift in energy $G^{j=1/2}(E) \approx G^{j=3/2}(E + E_{\mathrm{so}})$. The same shift applies to the phase shifts δ_{l_n,m_s}^c, so

$$\mu^M(E) \approx \mu_{j^+}^M(E) - \mu_{j^-}^M(E - E_{\mathrm{so}}). \tag{21}$$

This expression can be used to estimate the XMCD far from the edge for elements like Mn, and again predicts an effect proportional to $1/k$ and an additional $\pi/2$ phase shift.

III. CALCULATION FOR GD

We have carried out calculations of the XMCD for polycrystalline Gd in the EXAFS region based on the curved wave expression in Eq. (18) using several exchange models discussed below. We neglect the spin polarization of valence s, p, and d electrons, and assume that all seven f electrons have spin up for all Gd atoms. We have verified that the overlapped atom potential used in FEFF gives to very high accuracy, the same spin-up and -down densities as the self-consistent, full potential band-structure calculations of Albers and Ormeci.[17] We took σ^2 from the correlated Debye model[14] with $\Theta_D = 176$ K and $T = 150$ K. We ignored many body amplitude corrections, i.e., we set $S_0^2 = 1.0$, which is usually accurate to about 20%.[18] Atomic absorption coefficients were normalized at $k = 12$ Å^{-1} to circumvent absorption variations close to the edge. The results are compared with the experimental data of Schütz *et al.*,[16] both with and without the magnetic background subtracted. The overall normalization of experimental XMCD signal depends on many additional experimental factors: the degree of polarization of the x-ray beam, the amplitude reduction due to monochromators, the angle between the photon beam and the magnetization axis, and the degree of sample magnetization at a given temperature. The energy shift E_0 for all calculated exchange models was fixed by matching the calculated and measured peak at 78 eV above threshold in the XAFS signal (Fig. 1). The shifts

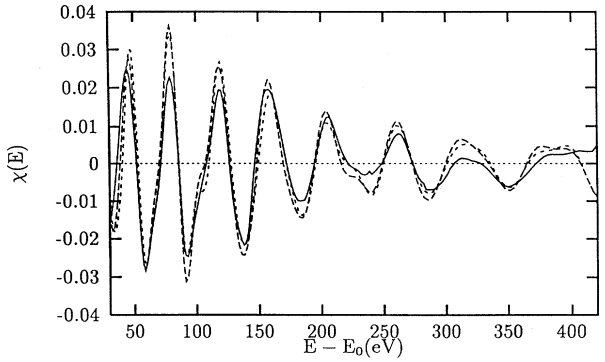

FIG. 1. Gd L_2 XAFS spectra. Comparison of experimental (solid) with calculated spectra using Hedin-Lundqvist (dashes) and Dirac-Hara (short dashes) self-energy models vs energy relative to the L_2 edge. Calculated spectra were energy shifted to match experimental peak positions.

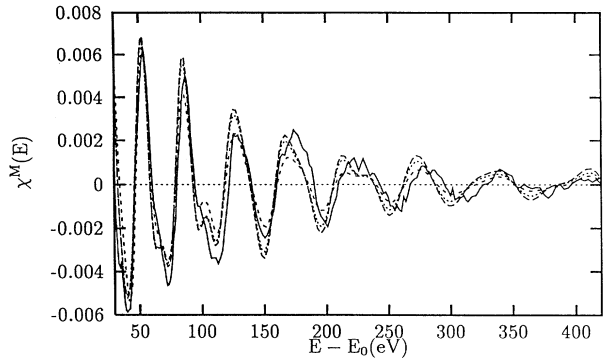

FIG. 2. Gd L_2 CPXAFS with background subtraction: comparison of experimental (solid) and calculated spectra for the three models discussed in the text with the same energy shifts were made as for the XAFS spectra of Fig. 1. Dashes, short dashes, and dots denote the modified-Von Barth-Hedin, -Dirac-Hara; and -Hedin-Lundqvist exchange-correlation models, respectively.

needed were 11 eV for the Hedin-Lundqvist and 5 eV for the Dirac-Hara self-energy models used in FEFF.[18] We used the same energy shift for the corresponding CPXAFS calculation using Eq. (18); thus no additional free parameters were needed or used in the XMCD calculations. For simplicity we only used paths with a half-total path length less than fourth-nearest-neighbor distance, $R_{\max} = R_{\rm tot}/2 = 7.29$ Å; the number of significant inequivalent paths up to this distance is 65. This number is sufficient to illustrate the magnitude of the XMCD effect and much of the fine structure. The sign of the XMCD signal depends on convention; our choice agrees with that of Schütz *et al.*[16]

As discussed above, a quantitative treatment of XMCD depends on the choice of exchange model, several of which were considered in our calculations:

(1) Modified Von Barth-Hedin Exchange—The ground-state spin-dependent local-density approximation (LDA) exchange-correlation potential of Von Barth and Hedin (BH) $V_{\rm gs}^{\rm BH}(\rho,x)$,[19] where $x = \rho_\uparrow/\rho$. This model is frequently used in band-structure studies of near-edge XMCD. However, the model has several drawbacks. For example, the difference in exchange potentials between spin-up and spin-down states is independent of energy, while the effect of the exchange interaction should generally decrease with increasing energy. Moreover, the model does not account for inelastic losses (or mean-free-path damping). Thus we also added a contribution from the spin-independent Hedin-Lundqvist self-energy[20] $\Sigma^{\rm HL}(E,\rho)$, which gives a good approximation to inelastic losses in XAFS,[18]

$$V_{xc}(E,\rho,x) = V_{\rm gs}^{\rm BH}(\rho,x) + \Delta\Sigma^{\rm HL}(E,\rho), \tag{22}$$

where $\Delta\Sigma^{\rm HL}(E,\rho) = [\Sigma^{\rm HL}(E,\rho) - \Sigma^{\rm HL}(E_F,\rho)]$. The difference in $\Delta\Sigma$ ensures that V_{xc} reduces to ground-state exchange at the Fermi energy E_F.[18] Note (Fig. 2) that the calculated amplitude of the XMCD signal is in reasonable agreement with experiment in this case, but somewhat high at large energies.

(2) Modified Dirac-Hara Exchange—An exchange model which posesses both energy and spin dependence is the local Dirac-Hara (DH) self-energy.[18] Thus we tried DH exchange together with the imaginary part of the HL self-energy to account for losses,

$$\begin{aligned} V_{xc}(E,\rho,x) = {} & V_{\rm gs}^{\rm BH}(\rho,x) \\ & + [\Sigma^{\rm DH}(E,\rho,x) - \Sigma^{\rm DH}(E_F,\rho,x)] \\ & + {\rm Im}\,\Delta\Sigma^{HL}(E,\rho). \end{aligned} \tag{23}$$

With this model, the amplitude of the signal in the 100–350 eV region is too small, i.e., the DH exchange decays too rapidly with energy, owing to the neglect of dielectric screening. Also the DH self-energy often gives poor description of the XANES region.[18]

(3) Modified Hedin-Lundqvist Exchange—We also attempted to simulate both the energy and spin dependence with an *ad hoc* model, constructed to have the same energy dependence for the difference in potentials between spin-up and -down as the Hedin-Lundqvist self-energy and the same spin dependence as the potential of Von Barth and Hedin,

$$\begin{aligned} V_{xc}(E,\rho,x) = {} & V_{\rm gs}^{\rm BH}(\rho,x) + \frac{V_{\rm gs}^{\rm BH}(\rho,x)}{V_{\rm gs}^{\rm BH}(\rho,0.5)} \\ & \times [\Sigma^{\rm HL}(E,\rho) - \Sigma^{\rm HL}(E_F,\rho)]\,. \end{aligned} \tag{24}$$

This model gives the best amplitude vs energy dependence. But clearly a less *ad hoc* treatment of spin- and energy-dependent exchange is desirable. However, for all three tested exchange models the sign, amplitude, and general form of the CPXAFS signal agree reasonably well with experiment (Fig. 2). As noted by Von Barth and Hedin,[19] the spin dependence of the correlation energy is important and can reduce the exchange interaction by a factor of about 2. In Fig. 3 we show the calculated signal, including the smooth XMCD background, which we find

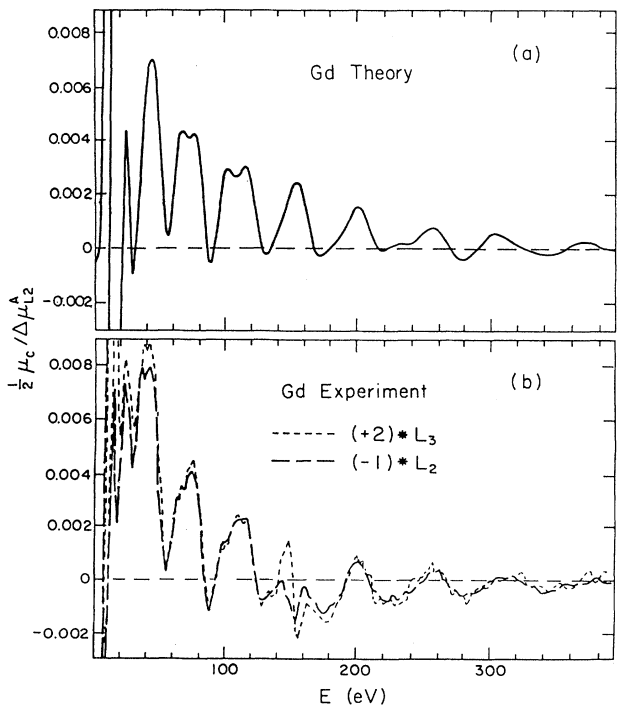

FIG. 3. Gd L_2, L_3 CPXAFS without background subtraction: comparison of (a) calculated spectra with the modified-Hedin-Lundqvist exchange (solid) and (b) experimental spectra (dashes). The calculated spectrum has the same energy shift as the XAFS spectra of Fig. 1.

to be essential to account for the observed XMCD behavior. Comparison with experimental data of Schütz *et al.*[16] shows good agreement with the calculated sign and amplitude of this background signal. Still the exchange interaction alone gives no XMCD signal at the L_1 edge of Gd,[16] whereas the significant amplitude of the observed XMCD L_1 signal for Gd suggests that there may be additional corrections at the L_2, L_3 edges from the same mechanisms that account for XMCD at $l = 0$ shells.

IV. SUMMARY AND CONCLUSIONS

A formal expression for the XMCD signal for half-filled shells has been developed into a form suitable for calculations based on a generalization of the MS XAFS and XANES code FEFF (version 6).[14] The dominant mechanism responsible for CPXAFS at the L_2 and L_3 edges is the spin- and energy-dependent exchange interaction of the photoelectron with the Fermi sea. The amplitude of the CPXAFS is roughly proportional to an effective magnetic scattering amplitude f_{eff}^{M}, which depends on the magnetization both of the scattering atom and the central atom. Since the theory for other than half-filled shells is more involved, the half-filled cases can provide a good test of various exchange potentials. All free parameters in the XMCD theory can be fixed by fitting XAFS theory to experiment. The results of our calculations of XMCD above the L_2 and L_3 edges of Gd are in satisfactory agreement with experiment, but differ somewhat between the various exchange models. This indicates that the main approximations made in derivation, namely the neglect of exchange splitting for core electrons and the SO interaction for the photoelectron are reasonable. However, *none* of the tested hybrid exchange models naturally accounts for the spin and energy dependence of the exchange interaction, including inelastic losses. The smooth atomic background XMCD signal predicted by our theory agrees well with that found in the experiment, illustrating the necessity of taking into account atomic matrix element factors in the theory.

ACKNOWLEDGMENTS

We are very grateful to G. Schütz, M. Knülle, and D. Ahlers for making their XMCD and XAFS data and details of their experiments available to us, and to the Freie Universität Berlin for hospitality during the early stages of this work. We also thank R. C. Albers, M. Altarelli, M. Alouani, K. Baberschke, H. Ebert, A. Fontaine, C. R. Natoli, H. Ormeci, P. Rennert, E. A. Stern, and especially C. Brouder for informative comments. This work was supported in part by US DOE Grant No. DE-FG06-ER45415-A003.

[1] J. L. Erskine and E. A. Stern, Phys. Rev. B **12**, 5016 (1975).
[2] G. Schütz, W. Wagner, W. Wilhelm, P. Kienle, R. Zeller, R. Frahm, and G. Materlik, Phys. Rev. Lett. **58**, 737 (1987).
[3] D. Gibbs, D. R. Harshman, E. D. Isaacs, D. B. McWhan, D. Mills, and C. Vettier, Phys. Rev. Lett. **61**, 1241 (1988); L. Baumgarten, C. M. Scneider, H. Petersen, F. Schäfers, and J. Kirschner, *ibid.* **65**, 492 (1990).
[4] B. T. Thole, P. Carra, and G. van der Laan, Phys. Rev. Lett. **68**, 1943 (1992); P. Carra, B. T. Thole, M. Altarelli, and X. Wang, *ibid.* **70**, 694 (1993); R. Wu, D. Wang, and A. J. Freeman, *ibid.* **71**, 3581 (1993).
[5] A derivation is given by A. Ankudinov and J. J. Rehr, Phys. Rev. B **51**, 1282 (1995); our spin-orbit sum rule (α) was previously derived by B. T. Thole and G. van der Laan, Phys. Rev. A **38**, 1943 (1988); and the sum rules for linear dichroism (γ, β) were derived by P. Carra, H. König, B. T. Thole, and M. Altarelli, Physica B **192**,182 (1993); see also, B. T. Thole and G. van der Laan, Phys. Rev. Lett. **70**, 2499 (1993).
[6] P. Carra, B. N. Harmon, B. T. Thole, M. Altarelli, and G. A. Sawatzky, Phys. Rev. Lett. **66**, 2495 (1991);
[7] H. Ebert, P. Strange, and B. L. Gyoffy, J. Appl. Phys. **63**,

3055 (1988); H. Ebert and R. Zeller, Phys. Rev. B **42**, 2744 (1990).
[8] U. Fano, Phys. Rev. **178**, 131 (1969).
[9] C. Brouder and M. Hikam, Phys. Rev. B **43**, 3809 (1991).
[10] C. Brouder, J. Phys. Condens. Matter **2**, 701 (1990); C. Brouder, M. Alouani, and K. H. Bennemann (unpublished).
[11] J. Goulon, Physica B **208&209**, 789 (1995); Y. Udagawa and M. Nomura, Jpn. J. Appl. Phys. **32**, Suppl. **32-2**, 284 (1993); L. Alagna, S. Di Fonzo, T. Prosperi, S. Turchini, P. Lazzaretti, M. Malagoli, R. Zanasi, C. R. Natoli, and P. J. Stephens, Chem. Phys. Lett. **223**, 402 (1994).
[12] B. Sinkovic and C. S. Fadley, Phys. Rev. B **31**, 4665 (1985).
[13] J. J. Rehr and R. C. Albers, Phys. Rev. B **41**, 8139 (1990).
[14] S. I. Zabinsky, J. J. Rehr, A. Ankudinov, R. C. Albers, and M. J. Eller, Phys. Rev. B **52**, 2995 (1995); J. J. Rehr, Jpn. J. Appl. Phys. **32**, Suppl. **32-2**, 8 (1993).
[15] A. Messiah, *Quantum Mechanics* (Interscience, New York, 1961), pp. 1056–1060.
[16] G. Schütz, R. Frahm, P. Mautner, R. Wienke, W. Wagner, W. Wilhelm, and P. Kienle, Phys. Rev. Lett. **62**, 2620 (1989); G. Schütz *et al.* (private communication).
[17] R. C. Albers and A. Ormeci (private communication); A. Ormeci, B. M. Hall, and D. L. Mills, Phys. Rev. B **42**, 4524 (1990).
[18] J. Mustre de Leon, J. J. Rehr, S. I. Zabinsky and R. C. Albers, Phys. Rev. B **44**, 4146 (1991).
[19] U. Von Barth and L. Hedin, J. Phys. C **5**, 1629 (1972).
[20] B. I. Lundqvist, Phys. Kondens. Mater. **6**, 206 (1967); L. Hedin and S. Lundqvist, *Solid State Physics: Advances in Research and Applications*, edited by F. Seitz and D. Turnbull (Academic, New York, 1969), Vol. 23, pp. 1–181.